JOURNAL OF APPLIED ELECTROCHEMISTRY 5 (1975) 177–185

*Measurement and regulation of oxygen content in selected gases using solid electrolyte cells. II. Differential gauge**

J. FOULETIER, H. SEINERA, M. KLEITZ

Laboratoire de Cinétique Electrochimique Minérale associé au CNRS (ERA No 384), E.N.S. d'Electrochimie et d'Electrométallurgie de Grenoble, Domaine Universitaire, 38401 St. Martin d'Heres, France

Received 6 August 1973

A differential arrangement has been used to study the equilibrium conditions between gases and electrodes in solid-state electrochemical oxygen gauges. At relatively low temperatures, the flux of oxygen from the reference to the analysed gas resulting from the electrolyte semipermeability is negligible as far as the oxygen content in the analysed gas is concerned but is still sufficient to disturb the equilibrium conditions near the electrode triple contact; noticeable errors are thereby introduced in the measurement of low oxygen partial pressures. Two new procedures are proposed for measuring very low oxygen partial pressures. By these procedures the Nernst and Faraday laws were verified with accuracies of the order of a few per cent for oxygen concentrations of less than 1 ppm in argon.

1. Introduction

According to estimates by Lindsay and Ruka [1] and Ullmann [2], oxygen-pressure measurements using solid electrolyte cells are accurate to within 2% when the oxygen pressures are higher than a few Torr. The scatter is mostly due to the error in measurement of cell temperature and knowledge of the electrolyte electronic conductivity. Thus neglecting an electronic transport number of about 0·5% introduces an error of 1·5% in an oxygen pressure of 1 Torr at 700°C.

When oxygen pressures are lower, the inaccuracy is greater. Etsell and Flengas [3] reported an inaccuracy of more than 30% for oxygen contents around 1 ppm in argon. According to Ulmann *et al.* [4], the Nernst law is not followed for oxygen concentrations less than 2 ppm when stabilized zirconia is used as an electrolyte. This inaccuracy is usually ascribed to an oxygen flow from the reference to the analysed gas through the electrolyte.

In this paper, results for oxygen gauges in the low-pressure range are analysed. Measurements were carried out using a design of differential gauges which is the subject of a patent [5].

2. Oxygen permeability of solid electrolytes

The permeability of ceramic, solid electrolyte is manifested by variation of the measured E.M.F. with flow rate of the analysed gas [3, 4, 6]. Hayes *et al.* [7] have noted that oxide ceramics often have a selective permeability to oxygen. Measurements by Ovchinnikov [8], Moebius [9], Fabre [10], and Ullman [11] have confirmed this and shown that it is advisable to distinguish a physical permeability and an 'electrochemical semipermeability' [12].

The physical permeability is the result of porosity and can be easily measured [13-15]. It is now possible to fabricate electrolytes for oxygen gauges for which this permeability is negligible as compared to the other, and this factor is neglected in the discussion below.

The electrochemical semipermeability results from the electronic conductivity of the electrolyte [16–31]. To a first approximation, it can be described as caused by an electronic shunt across the cell which results in the passage of ionic current through the electrolyte and a discharge of ionic carriers at electrodes to form or consume oxygen. The corresponding oxygen flux can be estimated

* Part III of this paper appeared in the previous issue of this journal.

by use of the theoretical equation due to Wagner [32, 33]:

$$\tilde{J} = -\frac{1}{16F^2L}\int_{\mu_1}^{\mu_2}\sigma_e t_{ion}\, d\mu_{O_2} \qquad (1)$$

where L is the electrolyte thickness, σ_e is the electronic conductivity, t_{ion} is the ionic transport number and μ_{O_2} is the oxygen chemical potential; μ_1 and μ_2 are the values of μ_{O_2} at the electrodes.

With solid electrolytes used in oxygen gauges, t_{ion} is close to 1 and the integral in Equation 1 can easily be calculated:

$$\tilde{J} = \frac{\bar{\sigma}_e}{4FL}E_{th} \qquad (2)$$

$$\tilde{J} \approx \frac{\bar{\sigma}_e}{4FL}E = kE \qquad (3)$$

where $\bar{\sigma}_e$ is the average electronic conductivity, E is the cell voltage, E_{th} is the theoretical E.M.F., and k is a function of temperature for a given cell. Equation 3 indicates that $\tilde{J}$ is proportional to $\bar{\sigma}_e$. So to minimize $\tilde{J}$ it is advisable to select an electrolyte with a low electronic conductivity.

From this point of view, the results by Ulmann *et al.* [4] seem to show that thoria might be a better electrolyte than zirconia when used under appropriate conditions. With thoria these authors verified the Nernst law at an oxygen content equal to 0·1 ppm in argon whereas with zirconia the limit is usually reached at about 1 ppm. Unfortunately, such data are very scarce and usually too inaccurate to distinguish the best electrolyte.

Several authors [8, 9, 22, 25] have shown that $\bar{\sigma}_e$ and $\tilde{J}$ increase exponentially with temperature. For temperatures higher than 1000°C, $\tilde{J}$ may be very important and could well have been the cause of the discrepancies observed in the use of gaseous references H_2-H_2O and CO-CO_2 [34]. Obviously $\tilde{J}$ can be minimized by lowering the cell temperature. As the cell impedance also increases exponentially as the temperature decreases, the compromise temperature is generally around 700–800°C.

Equation 3 also points to the proportionality of $\tilde{J}$ to E. To minimize the flux $\tilde{J}$, a reference atmosphere may be selected such that the cell voltage is small, and Wilson [35] proposed to adjust the pressure of a pure oxygen reference until the voltage is zero and then measure this pressure manometrically. Selecting various metal-metal oxide electrodes could also be used. However, a new difficulty is then created in the accurate measurement of the oxygen pressure in the reference atmosphere.

Another solution to this difficulty can be achieved by separating the reference atmosphere from the analysed gas so that no semipermeability flow of oxygen reaches the analysed gas, as proposed by Besson *et al.* [5] and by Sato [36]. We have carried out measurements on this type of cell. An alternative arrangement, involving two electrolytes in series, was studied for other purposes by Tretyakov and Muan [37], but the advantages of this cell have been questioned [38].

3. Basic diagram of the differential gauge

The differential gauge is composed of two regular gauges connected in series by an electrical contact as shown in Fig. 1. The gas spaces are denoted by

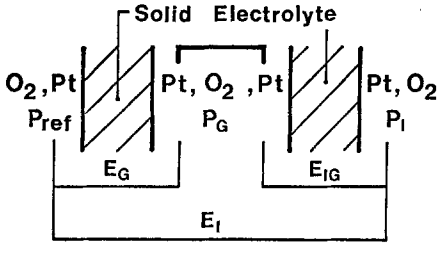

Fig. 1. Schematic diagram of the differential gauges.

'outer' where the oxygen pressure is P_{ref}, 'intermediate' (P_G) and 'inner' (P_I). Let E_G and E_{IG} be the actual voltages of the two cells:

$$E_I = E_G + E_{IG}. \qquad (4)$$

If E_G and E_{IG} obey the Nernst law:

$$E_I = \frac{RT}{4F}\ln P_G/P_{ref} + \frac{RT}{4F}\ln P_I/P_G \qquad (5)$$

$$E_I = \frac{RT}{4F}\ln P_I/P_{ref}. \qquad (6)$$

In these circumstances E_I is a straightforward measurement of the oxygen pressure, P_I, and is not dependent on the oxygen partial pressure P_G in the intermediate space. Then the cell-voltage does not depend on a change of P_G resulting from an oxygen flow from the reference to the guard atmosphere. Moreover, if P_G is close enough to P_I the oxygen flux between the corresponding atmospheres is negligible. Thus, by choosing an

intermediate oxygen pressure, P_G close to that measured, P_I, it is possible to eliminate any flow of oxygen to the analysed gas, while preserving the simplicity of the simple gauge arrangement.

For these conclusions to be valid there must be equilibrium between each gas phase and the corresponding electrode. However, because mass transport between electrodes of a cell is not always negligible, complete local electrode gas equilibrium cannot be expected. The measure and interpretation of the deviations from the Nernst law for differential gauges is the purpose of the present study.

4. Experimental set-up

4.1. Differential gauge (Fig. 2)

The differential gauge is an assemblage of two coaxial electrolyte tubes* ($ID = 21{\cdot}5$ mm, $OD = 25$ mm and $ID = 9$ mm, $OD = 12{\cdot}6$ mm) of yttria-stabilized zirconia (9 mol % yttria). According to the supplier, the main impurities are in wt.%; 0·12 SiO_2, 0·10 Fe_2O_3, 0·16 Al_2O_3, 0·11 TiO_2. The tubes were impervious to a helium leak test.

The electrochemical cell consists of the flat bases of the tubes whose inner and outer surfaces are metallized. Metallic paints of silver or platinum† form the electrodes from which the organic binder was eliminated by firing at 850°C in air. Silver electrodes were used only in a few experiments. The remaining results presented were obtained with platinum electrodes. The electrical contact between the two cells was either silver or platinum powder, matching the electrodes. The various compartments were sealed by Viton O-ring joints. With the inner space at about 10^{-2} Torr, the pressure does not change noticeably over half an hour.

The gas for analysis is introduced into the inner tube, near the inner electrode, via an alumina capillary. A guard gas circulates continuously in the intermediate space. The outermost electrode is in contact with air which serves as a reference.

For voltage measurements, the electrodes were connected to a high-impedance input millivoltmeter‡ by insulated platinum leads. The temperature at the electrode surfaces was measured using

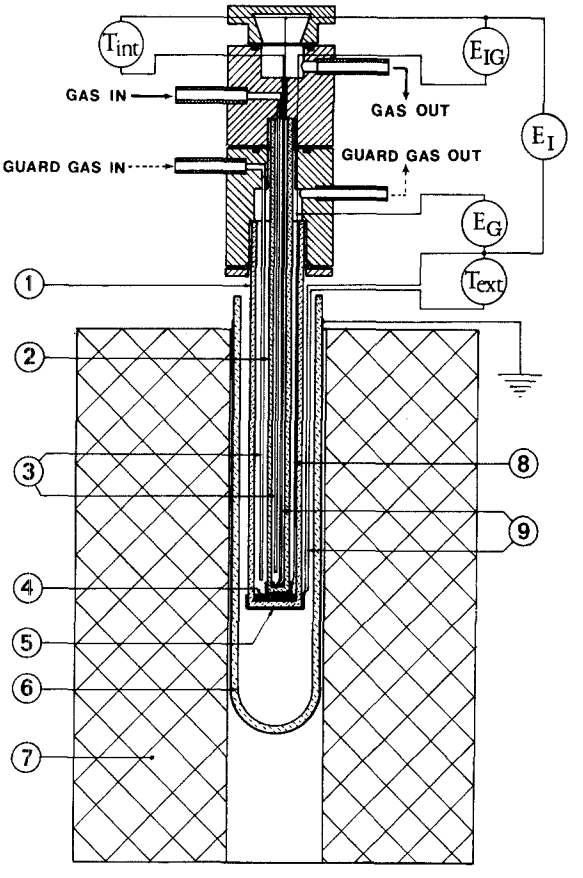

Fig. 2. Differential gauge. 1 – External electrolyte tube; 2 – inner electrolyte tube; 3 – alumina capillary; 4 – metallic powder (Pt or Ag); 5 – electrodes (Pt or Ag); 6 – alumina tube; 7 – electric furnace; 8 – platinum leads; 9 – Pt – Pt/10% Rh thermocouples.

thermocouples Pt–Pt 10% Rh derived from the same length of wire.

The cell was enclosed in a furnace having a high test capacity; the changes in cell-temperature were less than 1°C as were temperature differences between the electrodes. The cell was shielded against induced currents by a grounded platinum coating on an external alumina tube.

4.2. Gas circuits

This is shown in Fig. 3. The carrier gas was a nominally pure argon*, the oxygen content of which was regulated by an electrochemical pump [5, 39]. This gas circulated successively in the inner spaces of two identical differential gauges (DEG 1 and

* Zircoa tubes.
† Degussa 202 N and 308 A.
‡ Tacussel S 70/AS, $10^{12}\,\Omega$.

* Argon Air Liquide.

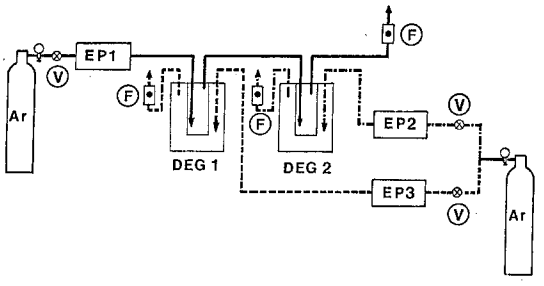

Fig. 3. Gas circuit. DEG 1 and DEG 2 are differential gauges; EP1, EP2 and EP3 are electrochemical pumps; V – valves; F – flowmeters.

DEG 2). Two similar gas circuits supplied oxygen-argon mixtures to the intermediate spaces of the gauges.

The flow rates were fixed by needle-valves and measured by rotameters. Accurate measurements were made to within 1% accuracy using a liquid-displacement flowmeter.

All the connecting tubes were of stainless steel and all joints of Viton.

5. Procedure

The initial experiments were designed to verify the properties described in Section 4. The total voltage E_I was measured with different oxygen pressures in the intermediate space of the first gauge DEG 1, with all other parameters being kept constant.

The temperature and flux of both the analysed and guard gases of the second gauge DEG 2 were kept constant during the measurements.

Any variations of the total voltage E_{I2} of the second gauge should detect any change in oxygen content in the analysed gas resulting from operations performed on the first. Prior to the experiments the random variations of E_{I2} were smaller than 0·5 mV. Under these conditions DEG 2, whose working temperature was around 700°C, permitted the detection and measurement of variations in oxygen-content greater than 1% of the initial content for the whole range of oxygen pressure examined.

5.1. Results

Typical results are shown in Fig. 4. The oxygen pressures shown were deduced using the Nernst relationship:

$$P_I = P_{ref} \exp\left(\frac{4FE_I}{RT}\right) \quad (7)$$

$$P_G = P_{ref} \exp\left(\frac{4FE_G}{RT}\right). \quad (8)$$

Lower than 800°C no change of the oxygen content of the analysed gas was detected by the second gauge upon changes in P_G in the first. At temperatures higher than 800°C a noticeable change was observed. It increased approximately exponentially with temperature as can be expected in the case of semi-permeability. However, accurate measurements of the change in oxygen-content were not made because of the temperature gradient along the tube through which the oxygen was passing which would preclude any interpretation. The qualitative results obtained indicate a significant oxygen permeability across the stabilized zirconia tubes above 900°C. For example, the oxygen flux from air to a nominally pure argon circulating at 11 l h^{-1} increased the oxygen content in the argon to 50 ppm when the flat base of the electrolyte tube was at 935°C.

In the temperature range where no oxygen permeability was observed, the oxygen pressure deduced by application of the Nernst law still depended noticeably on the oxygen pressure P_G, especially with low values of P_G. This is in contradiction with the theoretical predictions expressed by Equations 5 and 6.

In Fig. 4, results corresponding to the value $P_G = 0{\cdot}2$ atm are shown. In this case, the inner electrolyte tube functions as a simple gauge with air as reference. Under such conditions, the oxygen pressure deduced from E_I by application of the Nernst law depends on the cell temperature even below 800°C where no changes in oxygen content were detected by the controlling gauge.

5.2. Interpretation

Below 800°C the results shown in Fig. 4 can be split into two domains: Range I, or high P_G, corresponding to pressures P_G higher than about 10^{-4} atm and Range II, of low P_G. Within Range I, log P_I is approximately linear with respect to log P_G and within Range II the dependence is approximately exponential.

An explanation for this behaviour can be found in the work of Fabry *et al.* [34], who stressed the

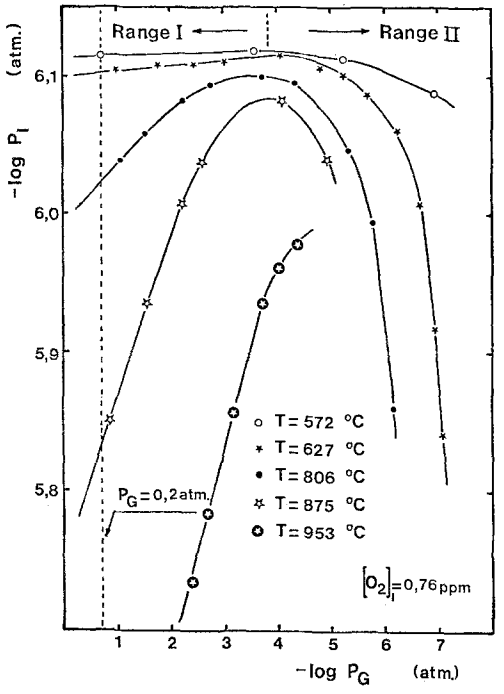

Fig. 4. Measured oxygen pressures deduced from the total voltage E_I using the Nernst law [7] as a function of the oxygen pressure in the intermediate space (with platinum electrodes).

need to consider the potential of an electrode as a measurement of the oxygen-chemical potential in a microsystem located around the electrode triple contact. Under certain conditions, especially low oxygen pressures, the oxygen exchange between this microsystem and the surrounding atmosphere may be very slow. The chemical potential of oxygen in the microsystem then becomes very sensitive to any disturbance and is generally different from the corresponding value in the surrounding atmosphere.

Our results show that oxygen passes through the electrolyte tubes above 800°C. At lower temperatures these flows do not induce any observable change in the gas composition but can be sufficient to disturb the microsystems of the electrode.

In this case the differential gauge can be schematically represented as shown in Fig. 5. This scheme incorporates the formalism proposed in references [41, 34]. Generally, when the pressures P_{ref}, P_G and P_I are different, oxygen passes through the electrolyte walls as shown and no microsystem is in equilibrium with the corresponding surrounding atmosphere. Limiting cases result when P_G is close to P_{ref} or P_I.

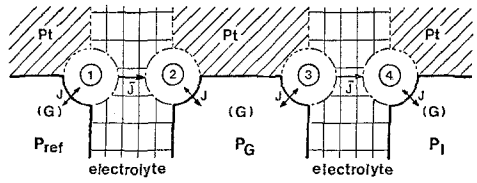

Fig. 5. Schematic diagram of the differential gauges following Fabry *et al.* [34].

The results of Kleitz *et al.* [40] showed that under high oxygen pressure there is a rapid exchange of oxygen between the electrode triple contact and the surrounding gas. It is therefore reasonable to assume that the microsystems 1, 2 and 3 are approximately in equilibrium with the corresponding gas when P_G is close to P_{ref}. In this case, departure from the Nernst law can be ascribed to a disturbance of the equilibrium conditions at electrode 4 which is the only electrode receiving a semipermeability flow of oxygen in contact with a low oxygen pressure.

When P_G is close to P_I, the semipermeability flow of oxygen between 3 and 4 is small and the induced disturbances of these microsystems can be neglected. Electrode 1 also is approximately in equilibrium with the reference atmosphere. Hence the departure from the Nernst law is mostly a consequence of the disturbance of microsystem 2.

An estimate of these deviations can be obtained by recourse to the simple model proposed by Kleitz [41]. According to this the oxygen-desorption flux from the microsystem is proportional to its atomic-oxygen concentration and the oxygen adsorption flux from the surrounding gas is proportional to the square root of its oxygen partial pressure.

At steady-state, the local oxygen flux resulting from the electrochemical semipermeability is equal to the net oxygen-rate exchange between the microsystem and the surrounding gas:

$$\tilde{J} = J_{des} - J_{ads}. \qquad (9)$$

From Equation 3 and the proposed model, this relation can be written:

$$kE = nC - m\sqrt{P} \qquad (10)$$

where n and m are supposedly independent of oxygen pressure.

The theoretical concentration C_{th} of atomic oxygen in the microsystem in absence of any disturbance is given by:

$$0 = nC_{th} - m\sqrt{P}. \quad (11)$$

If it is assumed that, in the investigated range of variation, the oxygen activity in the microsystem is proportional to its concentration C, the deviation δ of the electrode potential is given by:

$$\delta = \frac{RT}{2F} \ln \frac{C}{C_{th}} \quad (12)$$

or, according to the preceding equations:

$$\delta = \frac{RT}{2F} \ln \left(1 + \frac{kE}{m\sqrt{P}}\right). \quad (13)$$

The value of δ is small and can be approximated by the first term of the equivalent series expansion:

$$\delta = \frac{RT}{2F} \frac{kE}{m\sqrt{P}}. \quad (14)$$

Application of this general formula to the first case (P_G close to P_{ref}) yields a departure, δ_4:

$$\delta_4 = \frac{RT}{2F} \frac{k}{m\sqrt{P_I}} (E_I - E_G). \quad (15)$$

Here E_I can be regarded as approximately constant and P_I is a constant. Hence δ_4 is a linear function of E_G only.

In the second case (P_G close to P_I) the departure is:

$$\delta_2 = \frac{RT}{2F} \frac{k}{m\sqrt{P_G}} E_G. \quad (16)$$

P_G is approximately related to E_G by the Nernst law [8]. Therefore δ_2 can be expressed as a sole function of the parameter E_G by the equation:

$$\delta_2 = \frac{RT}{2F} \frac{kE_G}{m\sqrt{P_{ref}}} \exp \frac{(-2FE_G)}{RT}. \quad (17)$$

Equation 15 is applicable to the linear part of the plot observed in Range I and Equation 17 to the other part in Range II.

5.3. Experimental verification of the model

The arguments just developed allow us to neglect the deviations δ_1 and δ_3 associated with electrodes 1 and 3 in all cases (cf. Fig. 5). The measured voltage E_I can be expressed as:

$$E_I = E_{th} + \delta_2 + \delta_4 \quad (18)$$

where E_{th} is a constant given by the Nernst law of Equation 6. This can be simplified by writing:

$$e_I = E_{th} + \delta_4. \quad (19)$$

When P_G is close to P_{ref}, δ_2 is negligible and e_I is then equal to E_I. We have verified experimentally that E_I is a linear function of E_G in agreement with Equation 15 and that δ_2 given by:

$$\delta_2 = E_I - e_I \quad (20)$$

follows Equation 17.

Fig. 6 shows an example of the variation of E_I as a function of E_G. Within Range I, E_I is a linear function of E_G.

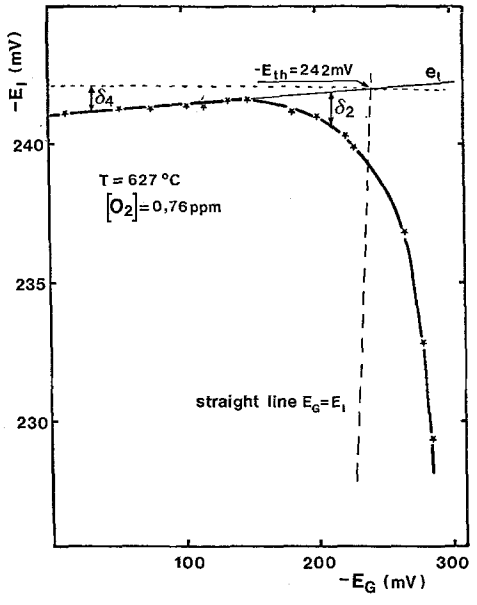

Fig. 6. Determination of E_{th} and definition of δ_4 and δ_2 (see text).

Fig. 7 gives an example in which Equation 17 is verified. The e_I values used for the calculation of δ_2 (cf. Equation 20) are deduced by extrapolation from the straight line, $e_I = E_I = f(E_G)$, drawn within Range I (cf. Fig. 6). Curves as shown in Figs. 6 and 7 were plotted at different temperatures and under different oxygen pressures P_I. The fact that Equations 15 and 17 were always verified substantiates the simple proposed model. Further experimental verifications are presented below.

The influence of the flow rate of the guard gas and the nature of the electrodes when all other parameters are kept constant have also been examined. The guard-gas flow rate has practically no influence on the total voltage E_I. Thus, with a

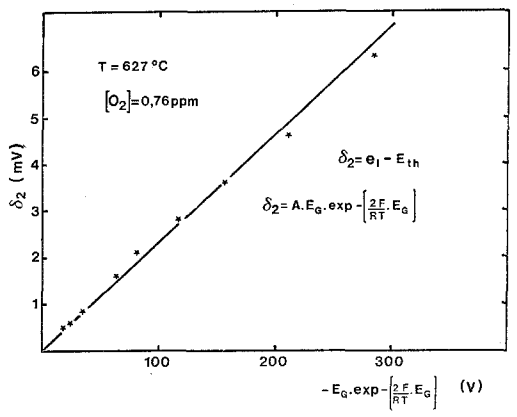

Fig. 7. Variation of δ_2 as a function of E_G.

pressure P_G of $1{\cdot}5 \times 10^{-5}$ atm and P_I of $0{\cdot}5 \times 10^{-6}$ atm, changes in the flow rate from 2 to 15 l h^{-1} do not induce variations of E_I greater than 0·5 mV although departure from the theoretical value is equal to about 11 mV under these circumstances. This shows that guard-gas turbulence has practically no influence and that this gas therefore has a homogeneous composition. Under these conditions, deviation from equilibrium concentrations shown by the observed departures from the ideal Equations 5 and 6 are necessarily located near the electrode triple contact.

With silver instead of platinum as the electrode metal, these phenomena are much more clearly marked and the steady-state conditions reached more slowly. These results can be understood by taking into account the high solubility of oxygen in silver. Because of this, the oxygen exchange reactions between the electrode triple contact and the surrounding atmosphere involve a diffusion of oxygen within the metal in addition to the absorption process which seems to be the only stage of importance with platinum.

This diffusion process is likely to cause an additional oxygen concentration gradient in series between the gas phase and the electrode triple contact.

6. Accurate measurement of low oxygen partial pressures by means of a differential gauge.

The first set of data presented in Section 4 emphasizes the requirement that the gauge operates within a temperature range where there is no change of oxygen content resulting from the electrochemical semipermeability. It is sufficient to operate the gauge at an adequately low temperature, i.e. lower than 800°C with the electrolytes used.

6.1. Measurement procedures

Considering the plots shown in Fig. 5 and their interpretation, two procedures can be employed within the low-temperature range. An approximate procedure consists in choosing the maximum E_{Imax} of the plot shown in Fig. 4 as the closest estimate of E_{th}. Experimentally, only one measurement is needed with a pressure P_G around 200 ppm because the maxima of such plots are always found close to this pressure. All measurements performed using this procedure have given oxygen pressures within 5% of the value determined by the alternative procedure. This is based on Equations 15 and 19. These show that e_I is equal to E_{th} when E_{IG} is zero. Experimentally, this point can be satisfied as follows (see Fig. 8). The straight line $e_I = f(E_G)$ is determined by two points corresponding to air in the intermediate space and with argon

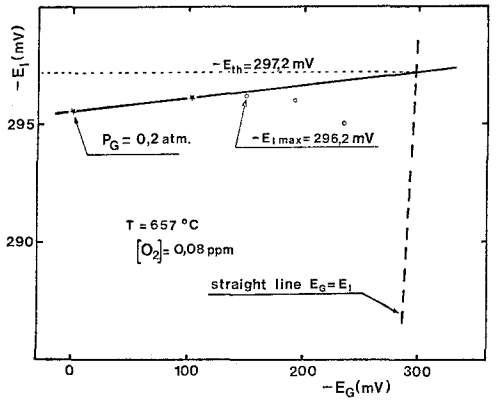

Fig. 8. Measurements of a low oxygen pressure according to the two proposed procedures.

containing 1000 ppm of oxygen. Under these conditions e_I is equal to the measured voltage E_I.

The point $e_I = E_{th}$ is at the intersection of the straight line previously determined and the locus corresponding to the condition $E_{IG} = 0$. In an E_I–E_G diagram, this locus is the first bisectrix, the equation of which is $E_I = E_G$.

6.2. Experimental verification

To confirm the merits of the proposed procedures

and consequently the models from which they derive, it has been shown that the Nernst and the Faraday laws are followed even when the oxygen contents are lower than 1 ppm if measurements of the oxygen pressures are made according to these procedures.

In the case of the Nernst law, an experimental set-up similar to the one described in Section 4.2 was used. The controlling gauge established that the oxygen content in the analysed gas was kept strictly constant during all the temperature cycles undergone by the investigated gauge DEG 1. Measurements were performed using the approximate procedure (with P_G close to 200 ppm). With an oxygen content of 0·68 ppm (Fig. 9) the Nernst law is followed only between 550 and 700°C (Fig. 10). The change in oxygen content resulting from the electrochemical semipermeability appears at 800 instead of 850°C.

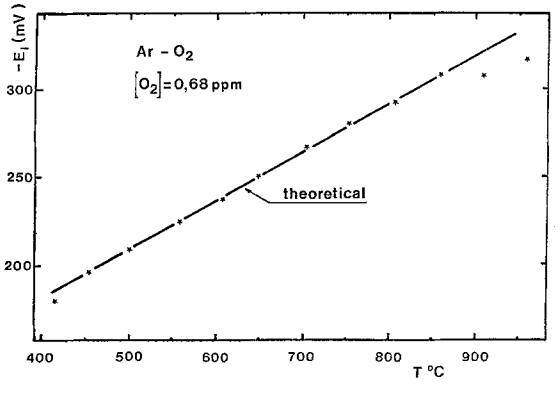

Fig. 9. Verification of the Nernst law with argon containing 0·68 ppm of oxygen.

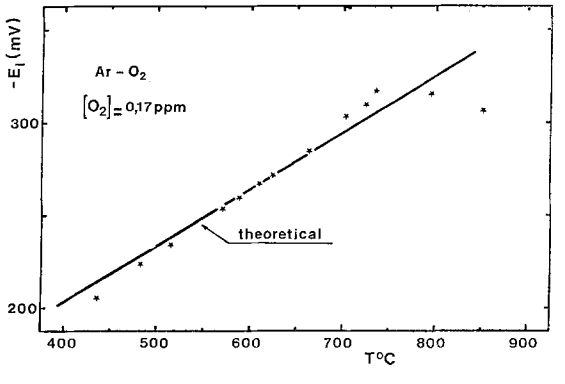

Fig. 10. Verification of the Nernst law with argon containing 0·17 ppm of oxygen.

law is closely followed within a broad range of temperature (450–850°C). Above 850°C, a divergence from the Nernst law is observed; in this case the controlling gauge indicates a change in the oxygen content. With an oxygen content of 0·17 ppm, the

The validity of Faraday laws was studied in a temperature range (500–700°C) where the Nernst law is well obeyed. A differential pump-gauge [5], based on the same principles as the differential gauges was used. This consists of two coaxial tubes of electrolyte whose composition is (ZrO_2) 0·91 (Y_2O_3) 0·09. The analysed gas was circulated inside the inner tube and a guard gas between the two tubes. The oxygen content of the latter was around 200 ppm. Surrounding air was used as reference. The analysed gas circulated successively in the differential pump-gauge, in the studied gauge DEG 1 and then in a flow meter whose accuracy is 1% (measured by displacement of liquid).

According to the Faraday law and previous calculation [42] the oxygen partial pressure P_I in the analysed gas is a function of the total current I which passes through the pump.

$$P_I = P_I^o \pm 3{\cdot}49 \times 10^{-3} \frac{IP}{D} \qquad (21)$$

where P_I^o is the initial oxygen partial pressure ($I = 0$); P is the total pressure; I is the current in mA and D is the flow-rate in $cm^3 min^{-1}$ at 0°C and 1 atm.

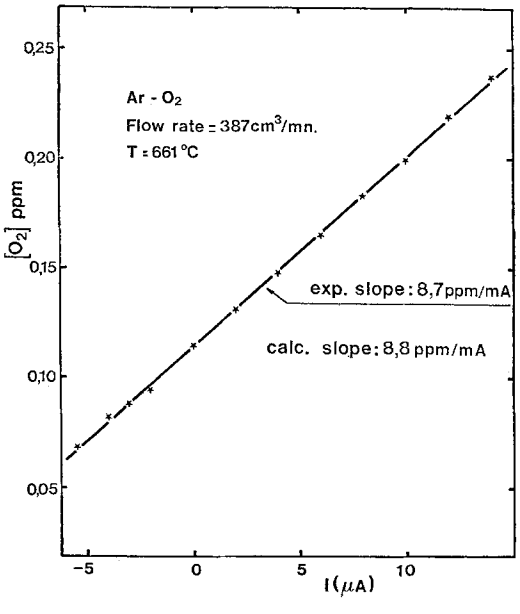

Fig. 11. Verification of the Faraday law.

Measurements of P_I were made using the approximate procedure. Fig. 11 shows an experimental result at 661°C with oxygen levels lower than 0·3 ppm. The linear variation of P_I versus I is well verified. The agreement between the experimental and the theoretical slopes deduced from the measured flow-rate by using Equation 21 is also very good if we take into account the inaccuracy of the flow-rate measurement.

7. Conclusion

The data presented have shown that the differential arrangement permits the use of solid-state oxygen gauges at very low partial pressures and greatly increases the accuracy of measurement in the low pressure range. The data support the model proposed by Fabry *et al.* [34] which emphasizes the easy disturbance of equilibrium electrode conditions at low pressures and the fact that variations of the chemical potential of oxygen can appear elsewhere than in the gas phase near the electrode triple contact. This last point clearly demonstrates that the absence of a voltage variation with change in the gas flow-rate in normal gauges is insufficient to ensure a correct measurement.

Acknowledgement

The authors are greatly indebted to R.A. Rapp for fruitful discussions.

References

[1] W.T. Lindsay and R.J. Ruka, *Electrochemica Acta* **13**, (1968) 1867.
[2] H. Ullmann, *Z. Phys. Chem. (Leipzig)* **250**, (1972) 195.
[3] T.H. Etsell and S.N. Flengas, *Met. Trans.* **3**, (1972) 27.
[4] H. Ullmann, D. Naumann and W. Burk, *Z. Phys. Chem. (Leipzig)* **237**, (1968) 337.
[5] J. Besson, M. Bonnat, C. Deportes and M. Kleitz, Fr. Addn. Prov. No 70, 38, 365; 23 Oct. 1970.
[6] J.B. Clegg, *J. Chromatogr.* **52**, (1970) 367.
[7] D. Hayes, D.W. Budworth and J.P. Roberts, *Trans. Brit. Ceram. Soc.* **60**, (1961) 494.
[8] Y.M. Ovchinnikov, S.V. Karpachev, A.D. Neuimin and S.F. Pal'guev, *Ogneupory* **30**, (1965) 40.
[9] H.H. Moebius, *Z. Phys. Chem. (Leipzig)* **233**, (1966) 425.
[10] R. Fabre, Thèse de Spécialité, Grenoble, July 1967.
[11] H. Ullmann, *Z. Phys. Chem. (Leipzig)* **237**, (1968) 71.
[12] J. Besson, C. Deportes and M. Kleitz, 'Piles Combust.', p. 87, Editions Technip Paris, 1965.
[13] G.M. Fryer, D.W. Budworth and J.P. Roberts, *Trans. Brit. Ceram. Soc.* **62**(1963) 525.
[14] H.H. Moebius and R. Hartung, *Silikat. Tech.* **16**, (1965) 276.
[15] W.A. Fischer and D. Janke, *Archiv. Eisenhuettenw.* **41**, (1970) 1027.
[16] J. Weissbart and L.S. Rowley, Electrochem. Soc. Meeting, Washington, 1964.
[17] A.W. Smith, F.W. Meszaros and C.D. Amata, *J. Am. Ceram. Soc.* 49, (1966) 240.
[18] E.W. Roberts, PhD. Thesis, Leeds, Sept. 1966
[19] R. Littlewood, *Canad. Metal. Quart.* 5, (1966) 1.
[20] A.A. Vecher and D.V. Vecher, *Dokl. Akad, Nauk Beloruss. SSR* **11**, (1967) 610.
[21] A.A. Vecher and D.V. Vecher, *Russ. J. Phys. Chem.* **41** (1967) 685.
[22] R. Hartung and H.H. Moebius, *Z. Phys. Chem. (Leipzig)* **243** (1970) 133.
[23] B. Korousic, *Rud. Met. Zb.*,2–3 (1971) 275.
[24] F.J. Salzano, H.S. Isaacs and B. Minushkin, *J. Electrochem. Soc.* **118** (1971) 412.
[25] P.A. Cherkasov, W.A. Fischer and C. Pieper, *Archiv. Eisenhuettenw.* **42** (1971) 873.
[26] R.A. Giddings and R.S. Gordon, *Electrochem. Soc. Meeting*, Houston, 1972.
[27] T. Reetz, *Z. Phys. Chem. (Leipzig)* **249**, (1972) 369.
[28] W.A. Fischer, *Archiv. Eisenhuettenw.* **39** (1968) 89.
[29] E. Foerster and H. Richter, *ibid*, **40** (1969) 475.
[30] W.A. Fischer and D. Janke, *Z. Phys. Chem. (F. am Main)*, **69** (1970) 11.
[31] R. Baker and J.M. West, *J. Iron Steel Inst.*, **204** (1966) 212.
[32] C. Wagner, *Elektrochem.*, **39** (1933) 543.
[33] C. Wagner: *Z. Phys. Chem.* **B21**, (1933) 25.
[34] P. Fabry, M. Kleitz and C. Deportes, *J. Solid State Chem.* **5**(1972) 1.
[35] H. Wilson, U.S. 3,442,773; 6 May 1969.
[36] M. Sato, 'Research Techniques for High Pressure and High Temperature', Chap. 3, G.C. Ulmer Edit., Springer Verlag, Berlin – New York (1971).
[37] J.D. Tretyakov and A. Muan, *J. Electrochem. Soc.* **116** (1969) 331.
[38] D.A. Shores and R.A. Rapp, *ibid*, **118** (1971) 1107.
[39] J. Besson, C. Deportes and M. Kleitz, Fr. Pat 1,580,819; 4 Aug. 1969.
[40] M. Kleitz, J. Besson and C. Deportes, 'Proceedings des deuxièmes Journées Internationales d'Etude des Piles à Combustible,' p. 354, Edit. S.E.R.A.I. – COMASI, Bruxelles, 1967.
[41] M. Kleitz, Thèse, Grenoble, May 1968.
[42] M. Kleitz, C. Deportes and P. Fabry, *Rev. Gen. Thermique* **97** (1970) 19.